AIAA 80-0993R

Installation Effects on Propeller Noise

H. K. Tanna,* R. H. Burrin,† and H. E. Plumblee Jr.‡
Lockheed-Georgia Company, Marietta, Ga.

The installation effects on propeller noise and propeller wake flow in flight have been examined experimentally by operating a model-scale propeller in the Lockheed anechoic open-jet wind tunnel. In particular, two aspects of propeller operation in a real situation have been quantified. These are: 1) the effects of nonzero angle of attack or propeller inflow angle relative to the flight path, and 2) the propeller inflow distortion due to the upwash generated by the presence of wing and flap behind the propeller. The results show that not only are these installation effects very important, but they are predicted inadequately using existing methods.

I. Introduction

As a result of some careful comparisons between the measured flight noise levels from propeller aircraft and the best predictions for propeller noise, it was observed at Lockheed about two years ago that while the comparison between measured and predicted noise levels is acceptable for some propeller/aircraft configurations, the noise levels produced by certain larger propeller/aircraft configurations (for example, the C-130 Hercules) are consistently greater than the predicted noise levels, the difference being of the order of 5-10 peak PNdB. Initially, it was thought that this "excess" noise could be attributed to other engine-related noise sources. However, the best estimates for these non-propeller noise sources indicated that in most cases, this explanation was not correct. It was therefore hypothesized (and the hypothesis turned out to be true, as will become apparent in this paper) that the observed discrepancies may be the result of propeller "installation effects."

When a propeller/engine configuration is mounted and operated on a real aircraft, the propeller noise can be expected to be modified due to at least three installation effects, compared to the noise generated from an isolated or uninstalled propeller operated at zero inflow angle. These installation effects are 1) the nonzero angle of attack or propeller inflow angle relative to the flight path, 2) the propeller inflow distortion due to the upwash generated by the presence of wing and flap behind the propeller, and 3) the additional noise generated by the interaction between the (highly turbulent and swirling) propeller slipstream and the wing/flap configuration. In the published propeller noise prediction methods, the last two installation effects are not included, and while some attempt has been made to predict the effects of propeller inflow angle on noise, the predictions have not been verified by adequate experimental results.

The primary objective of the work presented in this paper is to quantify these installation effects on propeller noise in flight by measuring the noise from a model-scale propeller operated in an anechoic open-jet wind tunnel.

In addition, in view of the current and projected energy shortages, it is essential to quantify the aerodynamic effects of the propeller slipstream on the performance of the wing. The extent of these interference penalties depends on the characteristics of the propeller wake, in particular on the swirl angles that directly influence the local angle of attack experienced by the wing. Since detailed measurements of swirl angles within a propeller slipstream are not available, the second objective of the present work was to conduct comprehensive surveys of wake flows behind propellers, and to compare the results with predicted slipstream properties, in particular the swirl angles.

The acoustic and aerodynamic measurements reported in this paper can be applied or extended to potential propfan designs which will become increasingly important in the future for fuel-efficient propulsion.

In the present paper, the facility and propeller model used to investigate installation effects on propeller noise and propeller wake flow are described in Sec. II. The main acoustic results are presented in Sec. III, while the highlights of the wake flow surveys are discussed in Sec. IV. Finally, Sec.V summarizes the major conclusions from this study and discusses some items of future work in this area.

II. Facility and Test Model

A thorough evaluation of the installation effects on propeller noise and propeller wake flow requires a rare combination of a well-controlled flight simulation facility and a highly versatile propeller test model. The present experiments were conducted in the Lockheed anechoic open-jet flight simulation facility, using a one-tenth scale Lockheed C-130 model propeller.

A. Anechoic Open-Jet Wind Tunnel

This facility is located in the Research Center of the Lockheed-Georgia Company. It is powered by a jet ejector, and is capable of providing continuous free-jet velocities up to 300 ft/s with a circular test section of 28 in. in diameter at the open-jet nozzle exit. A planview schematic of the facility is shown in Fig. 1. Air is drawn into the intake at the upper left through the honeycomb flow straightener and the screens to the contraction, across the open working (or test) section in the anechoic room, to the acoustically treated collector and diffuser, around the two right-angle corners fitted with acoustically treated turning vanes, and through the duct silencers to the exhaust section that contains the jet ejector (a long distance downstream and not shown in the figure). The entire exhaust section is lined with polyurethane foam from the anechoic room to just upstream of the ejector.

The anechoic room through which the open-jet test section passes is lined with 18-in. long polyurethane foam wedges and is anechoic at all frequencies above 200 Hz. It is 14 ft square in planform between wedge tips and is 20 ft high. The chamber is mounted on massive springs that isolate it from the rest of the building. A spring tensioned cable floor, suspended from the walls like a trampoline, provides easy access to the interior of the chamber for instrumentation and hardware changes and for calibration purposes.

The acoustic and aerodynamic characteristics of this facility have been thoroughly evaluated in the past, and the facility

Presented as Paper 80-0993 at the AIAA 6th Aeroacoustics Conference, Hartford, Conn., June 4-6, 1980; submitted July 23, 1980; revision received Oct. 22, 1980.

*Senior Scientist. Member AIAA.
†Associate Scientist.
‡Chief Scientist. Associate Fellow AIAA.

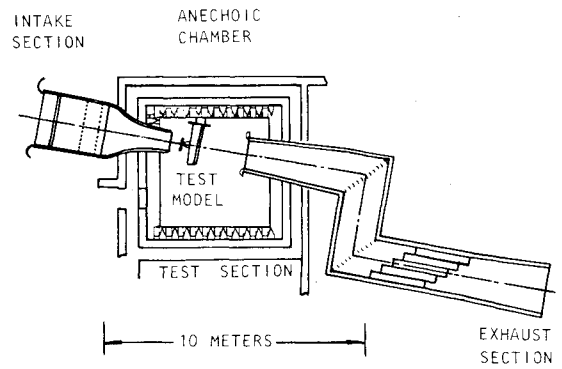

Fig. 1 Planview schematic of the Lockheed anechoic open-jet wind tunnel.

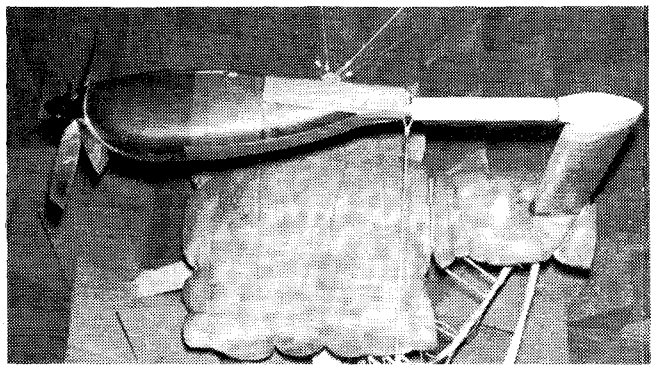

Fig. 2 Uninstalled propeller configuration, without wing and flap.

has been used in a number of projects, especially in the area of jet noise and airframe noise.

B. Propeller/Nacelle/Wing/Flap Model

The test model consists of the left outer wing panel of the C-130 one-tenth scale wind tunnel model with the outboard engine and propeller, suitably mounted to simulate propeller/nacelle and propeller/nacelle/wing/flap configurations. The propeller is one-tenth scale Hamilton Standard 54H60 right-hand rotation, with four blades and a diameter of 16.2 in. The blades have an activity factor of 175, and employ 16-series airfoil sections. The propeller is driven by a 50-horsepower (water-cooled) electric motor housed within the nacelle. The entire model was aligned with the tunnel flow using a low power laser.

Two series of experiments were conducted. In the first series, the propeller and nacelle were mounted in the test section using a sting support (i.e., without wing/flap), as shown in Fig. 2, to obtain "uninstalled" propeller noise levels. In the second series, the propeller/nacelle assembly was installed on the outboard section of the wing/flap of the exact one-tenth scale C-130 model, as shown in Fig. 3, thus providing "installed" propeller noise levels. In both configurations, the angle of attack α of the entire installation relative to the tunnel flow direction was varied from 0 to 10 deg. In addition, for each angle of attack, the measurements for the installed propeller were conducted at three flap settings, given by flap angles of $\gamma = 0$, 18, and 36 deg [which correspond to flap deflections of 0, 50 (takeoff), and 100% (landing approach), respectively, for the C-130 aircraft].

C. Facility/Test-Model Performance

One of the prime concerns studied at the beginning of these experiments was related to the aerodynamic performance of the facility/test-model combination. Since the 16.2-in. diam propeller was placed inside the potential core of the 28-in. diam open-jet test section, a possibility existed for some

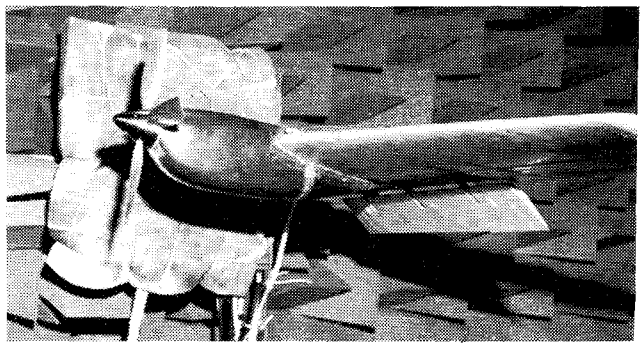

Fig. 3 Installed propeller configuration, with wing and flap.

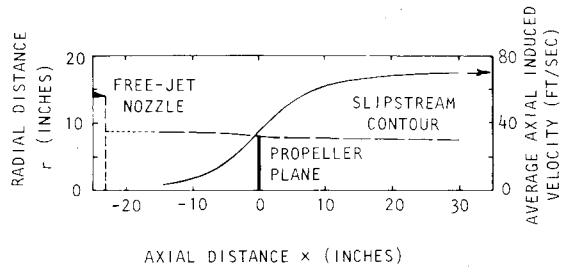

Fig. 4 Calculated characteristics of the propeller slipstream: $\beta_{0.75} = 35$ deg, $V_T = 255$ ft/s.

interference to occur between the propeller slipstream and the open-jet shear layer, in which case the main experiments would not be possible.

To investigate this problem, some theoretical calculations were first conducted, in which the properties of the propeller slipstream (in terms of its shape and induced velocities) were computed using an analytical technique, developed at Lockheed,[1] based on the vortex theory of propellers. A typical result for the exact test geometry considered in this study is presented in Fig. 4, which shows the propeller slipstream contour and the variation of average induced velocity as a function of axial distance in the test section. Two conclusions are worth noting from this figure. First, although the slipstream contracts with axial distance, the contour is contained well within the potential core of the test section, and, upstream of the propeller plane, it does not have the tendency to pull inward the flow from the boundary or edge of the open-jet potential core. Second, the average induced velocity at the open-jet nozzle exit plane is negligible, and, hence, the tunnel can be operated at the desired flow speed as if the propeller model were not present.

Although the theoretical conclusions just mentioned indicated that the aerodynamic interference between the propeller slipstream and the open-jet shear layer could be ruled out, it was decided to support these calculations with conclusive experimental evidence. Therefore, detailed axial mean velocity surveys were conducted using a multitube rake, positioned just behind the propeller, as shown in Fig. 5. The surveys were conducted in vertical as well as horizontal planes. A typical outcome is presented in Fig. 6, which shows a comparison of the mean velocity profiles in the test section with and without the propeller. It can be seen that, when the propeller is installed and operated in the test section, the tunnel or open-jet flow beyond the blade tip hardly is modified by the flow induced through the propeller disk. Hence, it was concluded that the facility can be used with confidence to evaluate the installation effects on propeller noise.

D. Experimental Conditions

All experiments were conducted at a tunnel speed V_T of 240 ft/s, with the propeller rotating at 10,200 rpm (i.e., ten times

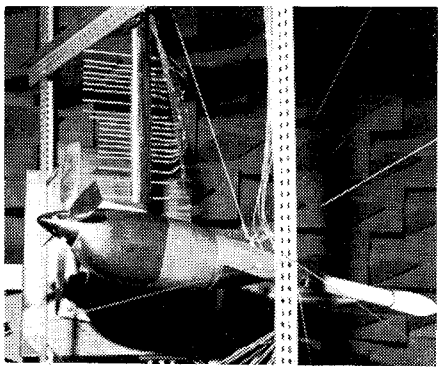

Fig. 5 Multitube rake for axial mean velocity measurements.

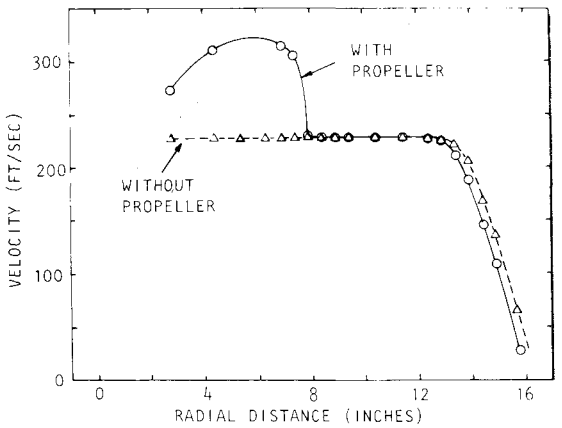

Fig. 6 Mean velocity profiles in the open-jet (or tunnel) test section.

the full-scale propeller rpm). This gives a blade tip speed of $V_t = 721$ ft/s (or $M_t = 0.64$), and the effective helical tip Mach number is $M_e = 0.674$. The blade pitch angle at the 75% radial station was kept constant at $\beta_{0.75} = 35$ deg. These values correspond to full-power takeoff conditions for the C-130 aircraft.

The noise measurements were conducted on two microphone arcs, one placed directly under the model (i.e., "overhead" plane) and the other located in a "sideline" plane, 30 deg below the horizontal plane through the model centerline. The microphones were placed at 10 deg intervals over the angular range from $\theta_m = 80$ to 150 deg relative to the *flight direction* (i.e., upstream axis), and the measurement distance, centered on the propeller hub, was 10 ft.

For each propeller noise test run, the corresponding background noise levels were obtained by removing the propeller and rotating the spinner at the test rpm, keeping all other test conditions identical. All results influenced significantly by background noise were not used in the data analysis. The propeller noise measurements were corrected for propagation through the open-jet shear layer. Although the noise sources in reality are distributed throughout the propeller disk, for the purpose of applying the open-jet shear layer corrections, the noise sources were assumed to be located at the center of the propeller disk for simplicity. Doppler frequency shifts were not applied to the measured data, and, hence, the final results refer to the situation in which the observer is moving *with* the propeller configuration relative to the stationary ambient medium.

The spectral results were analyzed in one-third octave bands as well as in narrowband form, using a constant analysis bandwidth of 40 Hz.

III. Acoustic Results

The major results from the acoustic experiments are described in this section.

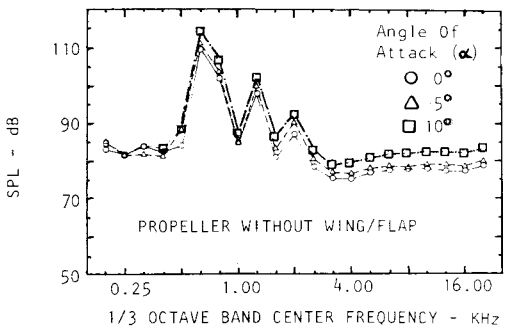

Fig. 7 Variation of propeller noise spectrum at $\theta_m = 90$ deg with angle of attack α.

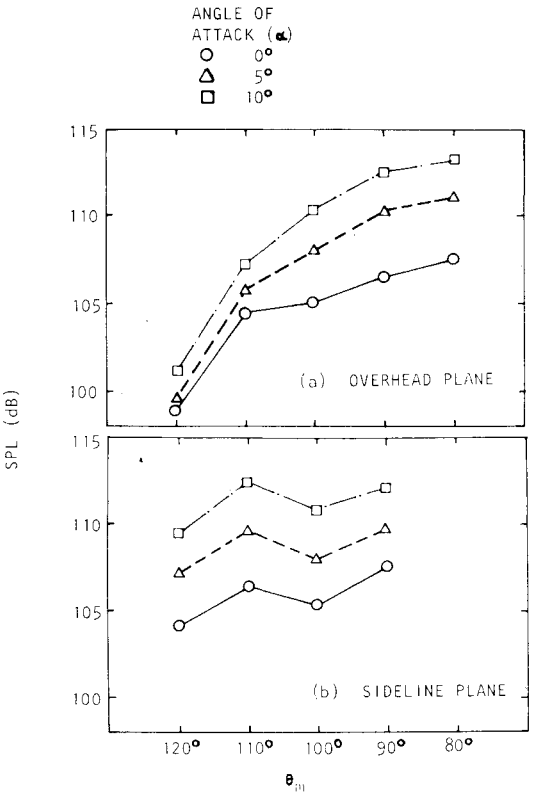

Fig. 8 Variation of discrete-frequency propeller noise (at the blade passage frequency) with angle of attack α: propeller with wing/flap, flap angle $\gamma = 18$ deg.

A. One-Third Octave Band Spectra

The effect of angle of attack α on uninstalled (i.e., without wing/flap) propeller noise spectrum at 90 deg in the overhead plane is shown in Fig. 7. The blade passage frequency throughout this test program is 680 Hz, and the first three discrete tones of propeller noise can be seen clearly in the one-third octave bands with center frequencies of 0.63, 1.25, and 2.00 kHz. The broadband noise dominates at frequencies greater than 5 kHz, with a broadband peak appearing around 10 kHz for the present model. As the inflow angle is increased from 0 to 10 deg, the whole spectrum increases almost uniformly in level by approximately 5-7 dB.

B. Discrete Frequency Noise

The installation effects on the discrete-frequency propeller noise at the fundamental blade passage frequency ($m = 1$) are shown in Figs 8 and 9. (The results at $m = 2$, not presented here, are also similar.) For the installed propeller (Fig. 8) with fixed flap angle ($\gamma = 18$ deg), the angle of attack α has a significant influence on the noise level at all angles, both in

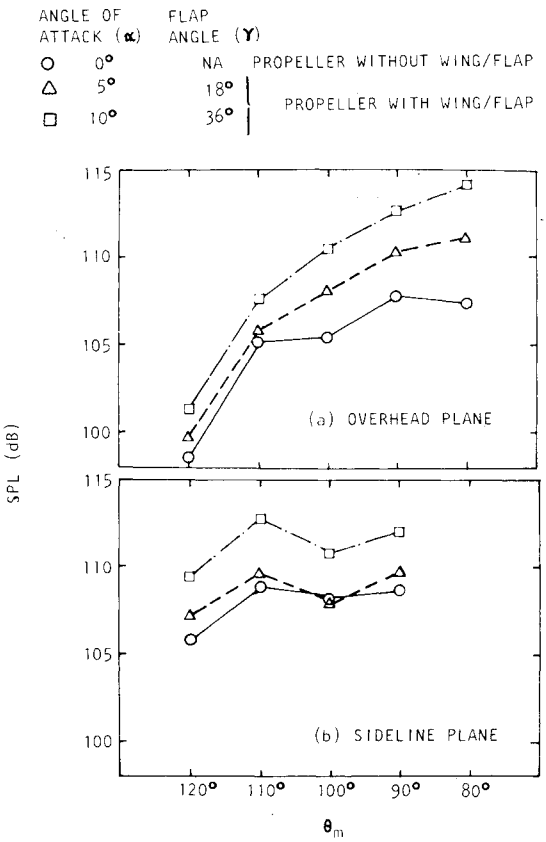

Fig. 9 Effect of installation on discrete-frequency propeller noise at the blade passage frequency.

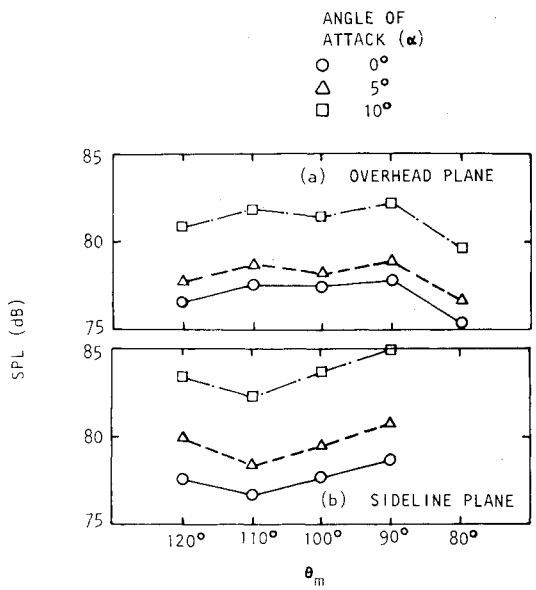

Fig. 10 Variation of peak broadband noise with angle of attack α: propeller without wing/flap.

the overhead plane and in the sideline plane. Typical comparisons between uninstalled and installed propeller noise levels are shown in Fig. 9, which demonstrates that an installed propeller with a nonzero angle of attack is significantly noisier than the isolated propeller at zero inflow angle relative to the propeller axis.

C. Broadband Noise

Similar plots for the levels in the 10 kHz one-third octave band, which, as mentioned earlier, is roughly the peak

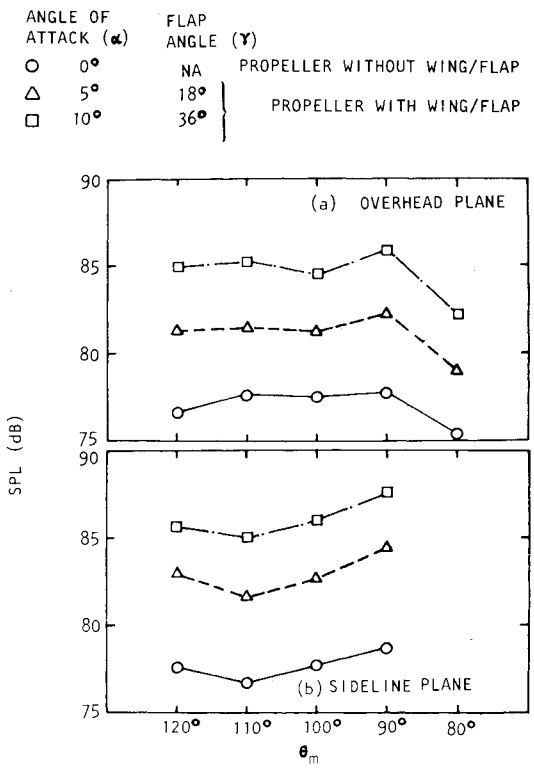

Fig. 11 Effect of installation on peak broadband noise.

frequency of the broadband noise for the present propeller, are given in Figs. 10 and 11. Here also, for the uninstalled propeller (i.e., without wing/flap), Fig. 10 shows that the noise levels in both overhead and sideline planes increase consistently and by significant amounts as the angle of attack is increased. In addition, a comparison of the results given in Figs. 10 and 11 shows that the noise levels increase even further if a wing with a deflected flap is present behind the propeller.

D. Comparison with Predictions

Some typical comparisons between measured and predicted levels of the discrete-frequency propeller noise at the fundamental blade passage frequency are shown in Figs. 12 and 13. In Fig. 12, the predictions have been obtained using a computer program published by Hamilton Standard,[2] whereas in Fig. 13, the predictions have been supplied by Farassat,[3-5] based on the work being conducted at NASA Langley. Unlike previous figures, the directivities in these two figures are expressed in terms of ψ, the "reception angle" (i.e., the observer angle relative to the flight direction when the sound is *received* by the observer).

In the first set of comparisons (Fig. 12), the measured directivity shapes in the overhead plane (Fig. 12a) are quite different from the predicted directivity shapes. Furthermore, around $\psi = 90$ deg, the measured levels increase as the angle of attack α increases, whereas the predicted levels shown an opposite trend. In the sideline plane (Fig. 12b), the measured and predicted directivity shapes are quite similar, although the effects of angle of attack are not predicted well, thus leading to large underprediction (6-7 dB) at $\alpha = 10$ deg. Similar discrepancies were also observed for the $m = 2$ comparisons, that are not included in this paper.

Using Farassat's prediction program (Fig. 13), the measured and predicted directivity shapes in the overhead plane (Fig. 13a) are a lot similar. In addition, at the peak radiation angle (around $\psi = 90$ deg), the predicted levels show roughly the correct amounts of increments as a function of angle of attack, although the absolute levels are being underpredicted by approximately 4-5 dB for all values of α. The

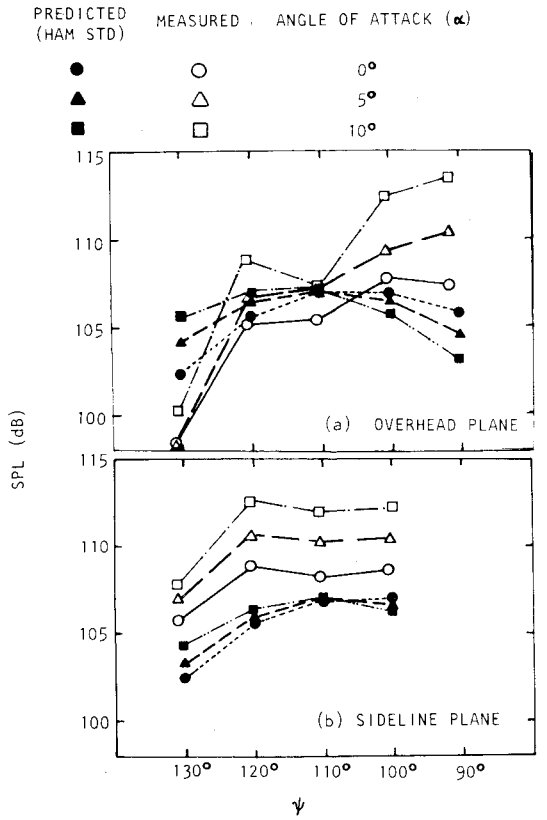

Fig. 12 Comparison between measured and predicted discrete-frequency propeller noise at the blade passage frequency: propeller without wing/flap.

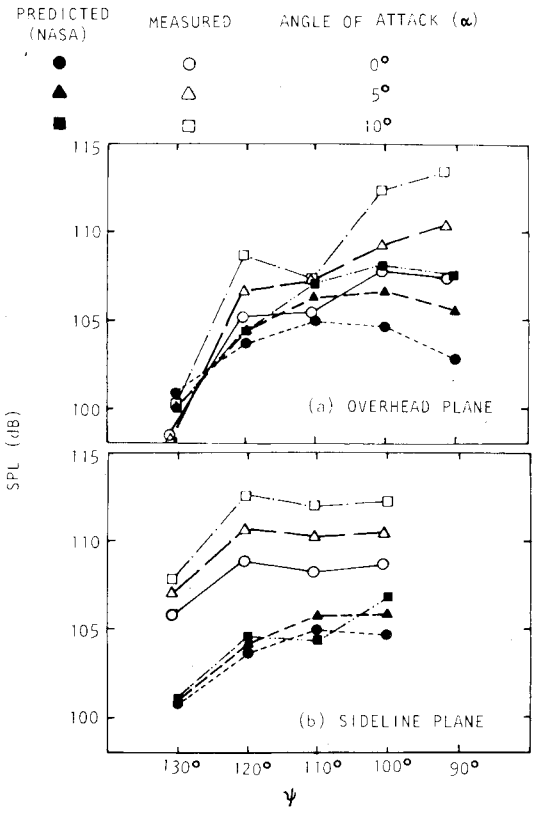

Fig. 13 Comparison between measured and predicted discrete-frequency propeller noise at the blade passage frequency: propeller without wing/flap.

comparison in the sideline plane (Fig. 13b), on the other hand, is not encouraging. Here, although the directivity shapes are being predicted quite well, the prediction scheme underestimates the measured noise levels by large amounts, especially as the angle of attack increases.

In Farassat's calculations, the effect on noise of any possible flow separation that may have occurred in the inner portion of the blades due to high angle of attack of the blade section (for $\alpha = 5$ and 10 deg) was not modeled, and this may be a possible reason for the observed discrepancies between measured and calculated results in Fig. 13.

IV. Propeller Wake Flow Measurements

The main purpose of the aerodynamic measurements was to determine the installation effects on flow through the propeller (i.e., axial velocity distributions, swirl angles, etc.), so that the measured flow changes can eventually be used 1) to explain the enhanced noise levels for installed propellers, and 2) to quantify the influence of the wake flow on wing performance. Due to the complex and time-consuming nature of these experiments, detailed measurements of propeller wake flows in flight have not been achieved with great success in the past.

A. Special Probe Rake for Flow Surveys

The propeller slipstream was mapped extensively, using a special seven-probe rake, with each probe having five miniature sensing holes, to measure the three-dimensional velocity components in a swirling flow. This probe rake has been calibrated fully at Lockheed in the past. The rake and support rod are shown in Fig. 14. The rake assembly was traversed automatically under computer control such that the surveys consisted of measurements on a grid of ½-in. squares. Surveys were made both with and without the propeller.

Using a special data processing program, the recorded pressure measurements were transformed to give the three components of the wake velocity, U (axial), V, and W, from which the swirl angles within the wake can be readily computed.

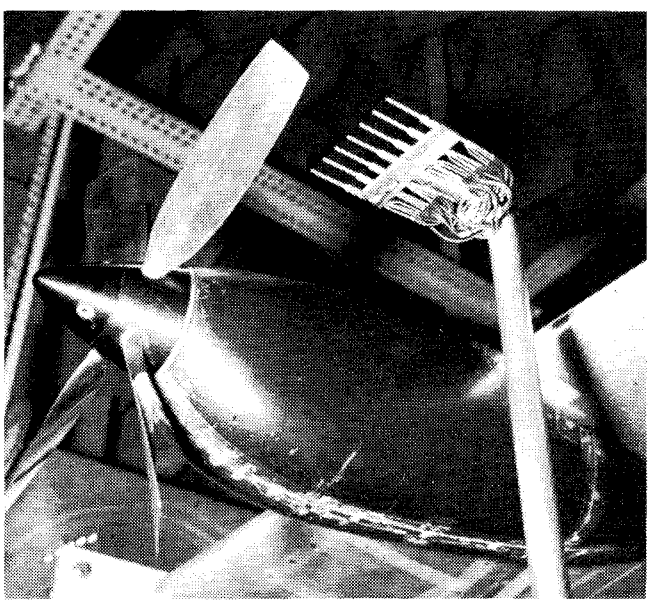

Fig. 14 Seven-probe (35-hole) rake for propeller wake flow measurements.

B. Highlights of Aerodynamic Measurements

The aerodynamic results were displayed in the form of contours and vector maps to provide a visual demonstration of the nature of the propeller wake. Figures 15-17 show typical results for the propeller/nacelle/wing/flap combination at zero angle of attack. In each figure, the blank area

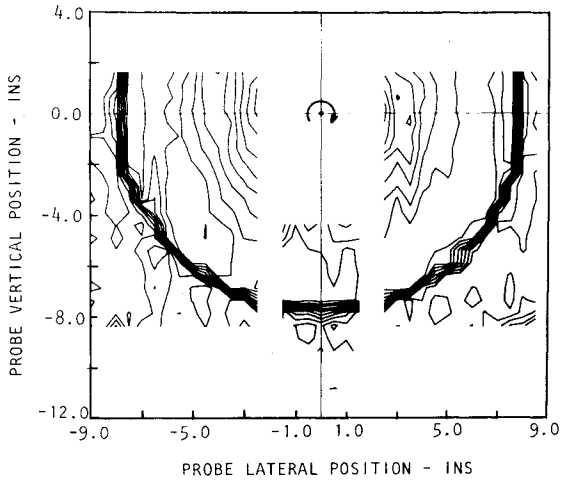

Fig. 15 Axial velocity contours (lines of constant U/U_0) behind propeller plane: propeller with nacelle and wing/flap, $\alpha = 0$ deg, $\gamma = 0$ deg.

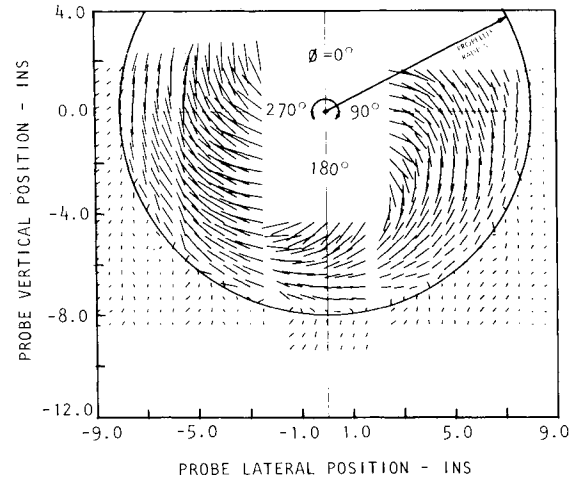

Fig. 16 Vector map of cross flow (V-W vectors) in propeller wake: propeller with nacelle and wing/flap, $\alpha = 0$ deg, $\gamma = 0$ deg.

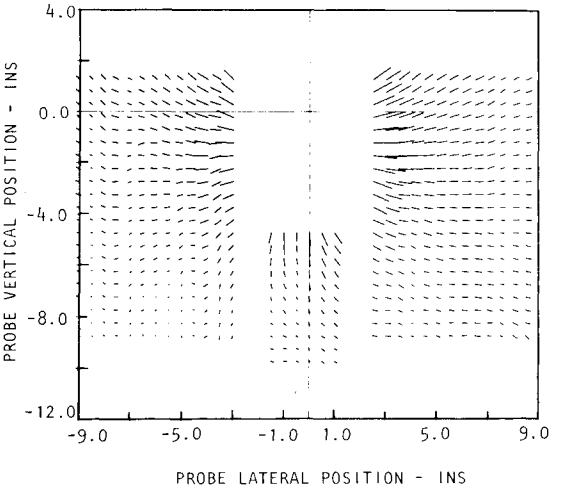

Fig. 17 Vector map of cross flow (V-W vectors) with propeller removed: nacelle with wing/flap, $\alpha = 0$ deg, $\gamma = 0$ deg.

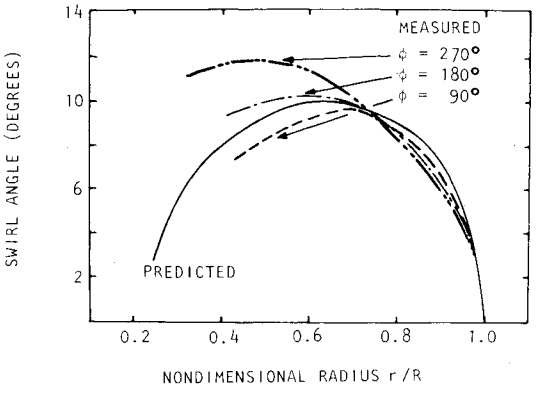

Fig. 18 Comparison of predicted and measured swirl angles.

in the middle represents the region over which measurements could not be obtained due to the presence of the nacelle.

The variation of the axial velocity U with radial distance is shown in Fig. 15 in contour form, where the velocity U is normalized by the freestream velocity U_0, and the contours are spaced $0.04U_0$ apart. At any radius, the axial velocity remains essentially constant with azimuthal position. Ideally, for an uninstalled propeller, the map would show concentric circles. The closely spaced contours near the blade tip indicate that the axial velocity changes rapidly as the blade tip is approached. The velocity gradually increases from the hub to reach a maximum value between the 0.8 and 0.95 radial station, after which it drops to "zero" (in fact, to the freestream value U_0) within a small distance. This distribution of axial velocity is a direct reflection of the blade loading distribution that can be used as input to the theoretical models for propeller noise.

The crossflow measurements with and without the propeller are shown as V-W velocity vector maps in Figs. 16 and 17, respectively. The straight lines effectively represent the vectorial sum of the tangential and radial velocity components. Its length represents the magnitude of the vector and its orientation represents the direction of the flow at that point.

Behind the propeller (Fig. 16), the tangential velocity that represents the swirl in the slipstream is clearly dominating. The radial velocity is generally weak and its contribution is appreciable only close to the nacelle. This vector map vividly marks the boundary of the slipstream, with no swirl outside this boundary. The slipstream diameter is slightly smaller than the propeller diameter, indicating a slight contraction. This contraction is expected because the survey was carried out a small distance downstream of the propeller plane. Outside the slipstream, the vectors indicate that there is a slight upwash due to the presence of the wing and flap. Within the slipstream, the swirl angles on the right side of the horizontal axis ($\phi = 90$ deg) are noticeably less than those on the left side ($\phi = 270$ deg). This difference is partly due to the upwash, which tends to oppose the tangential velocity at $\phi = 90$ deg and enhance it at $\phi = 270$ deg.

The presence of the nacelle is the second reason for this difference in swirl angle. As the nacelle is not axisymmetric, its shape tends to make it behave like a cylinder at a slight angle of attack. It induces a tangential velocity on its two sides, clockwise on the left and anticlockwise on the right as shown in Fig. 17. Although this induced velocity diminishes in magnitude with increasing distance from the nacelle sides, its effect in Fig. 16 is the same as that due to the upwash. That is, the swirl angle is reduced on the right and increased on the left.

C. Comparison with Theory

The propeller wake flow measurements obtained in this study were compared in detail with the analytical models based on the vortex theory of propellers under a separate research project at Lockheed.[1] A typical comparison of predicted and measured swirl angles is shown in Fig. 18. The

measured swirl angles are shown at three azimuthal angles, $\phi = 90$, 180, and 270 deg; as discussed earlier, the swirl angles at $\phi = 270$ deg are larger than the swirl angles at $\phi = 90$ deg, with the values for $\phi = 180$ deg falling somewhere between the two. The predicted swirl angles are shown by the full curve in the figure. Since the theoretical model (so far) does not include the effects of nacelle and wing (i.e., it assumes an isolated propeller), the predicted values are independent of azimuthal position, and, strictly speaking, they can be compared with measured values only in the $\phi = 180$ deg position, where the measured tangential velocities are not influenced by the upwash. The agreement between the measured and predicted swirl angles in this case is quite satisfactory at $\phi = 180$ deg.

V. Conclusions and Future Work

The installation effects of propeller noise and propeller wake flow in flight have been examined experimentally by operating a one-tenth scale C-130 model propeller (with and without a wing/flap section) in the Lockheed anechoic open-throat wind tunnel. In particular, two aspects of propeller operation in a real situation have been quantified and shown to be very important. These are 1) the effects of nonzero angle of attack or propeller inflow angle relative to the flight path, and 2) the propeller inflow distortion due to the upwash generated by the presence of the wing and flap behind the propeller. The major conclusions are as follows.

1) Both discrete-frequency and broadband noise levels from an "installed" propeller with nonzero inflow angle are significantly higher than the corresponding noise levels from an "uninstalled" propeller with zero inflow angle. The existing propeller noise prediction methods (considered in this investigation) do not account for these installation effects correctly, and significant improvements in the analytical models are required to achieve this.

2) The propeller wake flow characteristics, in particular the swirl angles induced by the propeller, are influenced significantly by the presence of the nacelle and the wing. The effect of the nacelle is more prominent at inboard blade stations.

Although the work described in this paper has highlighted the importance of installation effects on propeller noise and propeller wake flow properties, several specific items of work need to be conducted to improve the state-of-the-art in this area. These are as follows.

1) To verify that the model-scale noise data obtained in this study are directly applicable to the full-scale aircraft, the results need to be compared in detail with the C-130 flight noise measurements. This comparison will not only provide a unique verification of the size scaling laws for propeller noise, but it will also allow the propeller noise contribution to be separated from other engine-related noise sources on the C-130, which has not been done conclusively in the past.

2) The comparisons between measured and predicted noise levels reported here need to be extended to other existing prediction methods and theoretical models for propeller noise.

3) On a more fundamental level, although the experimental results obtained so far have shown conclusively that installation effects do lead to an increase in both the discrete-frequency and broadband components of propeller noise, the exact nature of the source(s) of increased (or additional) noise has not been identified. That is, while the increase in discrete tone levels may be logically attributed to the distortion of the propeller inflow due to the upwash generated by the wing and the flap, the increase in broadband noise may be due to either a) inflow distortion, or b) the additional noise generated by the impingement of the propeller slipstream on the wing/flap. To resolve these issues, the acoustic results need to be correlated with the corresponding wake flow measurements, using existing aerodynamic noise theories.

4) Finally, on the aerodynamic side, the prediction method considered in this study is strictly applicable to propellers with axisymmetric nacelles and zero angle of attack. To reflect azimuthal variation of slipstream properites due to nonzero inflow angle and nacelle/wing presence, these prediction methods need to be refined and also extended to include potential propfan configurations.

Work on some of the items listed is currently in progress at Lockheed.

Acknowledgments

This research was conducted with Lockheed internal funding. The authors gratefully acknowledge the contributions made by D. F. Blakney in conducting the wake flow measurements and in reducing both acoustic and aerodynamic data. The comparisons between measured and predicted propeller slipstream characteristics were done by A. S. Aljabri under a separate Lockheed internal research project.

References

[1] Aljabri, A. S., "Prediction of Propeller Slipstream Characteristics," Lockheed-Georgia Company Engineering Rept. LG79ER0120, Oct. 1979.

[2] Magliozzi, B., "V/STOL Rotary Propulsion Systems Noise Prediction and Reduction," FAA Rept. FAA-RD-76-49, May 1976.

[3] Farassat, F., "Theory of Noise Generation from Moving Bodies with an Application to Helicopter Rotors," NASA Tech. Rept. R-451, Dec. 1975.

[4] Farassat, F. and Succi, G. P., "A Review of Propeller Discrete Frequency Noise Prediction Technology with Emphasis on Two Current Methods for Time Domain Calculations," *Journal of Sound and Vibration*, Vol. 71, 1980.

[5] Nystrom, P. A. and Farassat, F., "A Numerical Technique for Calculation of the Noise of High Speed Propellers with Advanced Blade Geometry," NASA TP-1662, July 1980.